Dalton Transactions

Mechanistic insight into the ruthenium-catalysed anti-Markovnikov hydration of alkynes using a self-assembled complex: a crucial role for ligand-assisted proton shuttle processes.

Journal:	*Dalton Transactions*
Manuscript ID:	DT-ART-03-2014-000712.R1
Article Type:	Paper
Date Submitted by the Author:	24-Apr-2014

Complete List of Authors:	Slattery, John; University of York, Department of Chemistry Breit, Bernhard; Albert-Ludwigs-Universitat Freiburg, Institut fur Organische Chemie und Biochemie Gellrich, Urs; Albert-Ludwigs-Universitat Freiburg, Institut fur Organische Chemie und Biochemie Li, Timothy; University of York, Department of Chemistry Lynam, Jason; University of York, Department of Chemistry Milner, Lucy; University of York, Department of Chemistry Pridmore, Natalie; University of York, Chemistry Whitwood, Adrian; University of York, Department of Chemsitry

Note: The following files were submitted by the author for peer review, but cannot be converted to PDF. You must view these files (e.g. movies) online.

toc2.tif

Dalton Transactions

RSCPublishing

ARTICLE

Mechanistic insight into the ruthenium-catalysed *anti*-Markovnikov hydration of alkynes using a self-assembled complex: a crucial role for ligand-assisted proton shuttle processes

Cite this: DOI: 10.1039/x0xx00000x

Received ooth January 2012,
Accepted ooth January 2012

DOI: 10.1039/x0xx00000x

www.rsc.org/

This article is published in celebration of the 50th anniversary of the opening of the Chemistry Department at The University of York

Bernhard Breit,[b] Urs Gellrich,[b] Timothy Li,[a] Jason M. Lynam,[a]* Lucy M. Milner,[a] Natalie E. Pridmore,[a] John M. Slattery,[a]* and Adrian C. Whitwood.[a]

A combined computational and experimental study is presented that investigates the mechanism of the anti-Markovnikov hydration of phenylacetylene by $[Ru(\eta^5\text{-}C_5H_5)(6\text{-DPPAP})(3\text{-DPICon})]^+$ (where 6-DPPAP = 6-(diphenylphosphino)-N-pivaloyl-2-aminopyridine) and 3-DPICon = 3-diphenylphosphinoisoquinolone). The proposed mechanism, modelled using density functional calculations, involves an initial alkyne-vinylidene tautomerism, which occurs *via* a ligand-assisted proton shuttle (LAPS) mechanism. Intramolecular ligand assistance from the 6-DPPAP and 3-DPICon ligands, particularly the basic nitrogen of 6-DPPAP, is also involved in subsequent stages of the mechanism and three LAPS processes in total are observed. The self-assembled ligand backbone helps to create a water-binding pocket close to the metal centre, which facilitates nucleophilic attack of water at the vinylidene α-carbon and mediates protonation and deprotonation of subsequent acyl and vinyl intermediates. Experimental evidence is also presented for a novel non-productive catalyst deactivation pathway, which appears to arise from an initial lactam-lactim tautomerism of the 3-DPICon ligand followed by coupling with a vinylidene.

Introduction

Regioselective functionalisation is crucial in organic synthesis to allow the installation of functional-groups into simple carbon frameworks. Transition-metal catalysts are often excellent at promoting such reactions and in some cases these catalysts can rival the turnover frequency of nature's metalloenzymes. However, most synthetic catalysts rely primarily on metal centres to enable substrate transformations, whereas metalloenzymes may use both the reactivity and flexibility of metal centres and functional groups present on the protein backbone to facilitate catalytic reactions.

Some recent studies have attempted to use "bio-inspired" approaches in the design of new organometallic complexes and homogeneous catalysts, where functional groups present on the ligands play active roles alongside the metal in facilitating substrate transformation.[1] This synergy between non-innocent ligands and metal centres can be powerful and has been shown to effectively facilitate both stoichiometric and catalytic transformations in a range of studies. For example: ligand-assisted C-H activation is observed in the concerted metallation-deprotonation (CMD),[2] ambiphilic metal-ligand activation (AMLA),[3] ligand-assisted proton shuttle (LAPS) and ligand-to-ligand hydrogen transfer mechanisms.[4, 5] Ligand functionality is present in complexes of self-assembled pyridyl and imidazolyl phosphine ligand complexes and these functionalities have been associated with both the selectivity and activities of catalysts derived from them, with their activities sometimes being compared to enzyme systems.[6-9] This paper aims to gain insight into one of these enzyme-like organometallic catalyst systems, one which has been demonstrated to catalyse the *anti*-Markovnikov addition of water to terminal alkynes.[10]

Traditional terminal alkyne hydration methods involve either strong acid catalysts and Hg (II), or transition metal salts, and exclusively produce the Markovnikov-addition product (a methyl ketone). *Anti*-Markovnikov alkyne hydration has been accessible through stoichiometric hydroboration, or hydrosilylation, followed by oxidation, but these are stoichiometric processes and generate significant amounts of

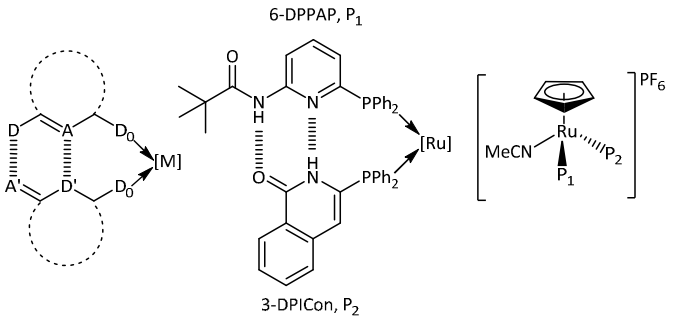

Figure 1: Self-assembled ligand hydrogen bonding creates a pseudo-bidentate system. The self-assembled ruthenium catalyst of interest to this study is shown to the right.

by-products during the reaction. In 1998, the first ruthenium-catalysed *anti*-Markovnikov terminal alkyne hydration was reported by Tokunaga and Wakatsuki and the mechanistic features of this system were subsequently explored.[11] Following on from their work, many ruthenium catalysts have been developed to improve the selectivity, activity and stability of these systems.[1]

One of the most recent developments in the field of *anti*-Markovnikov terminal alkyne hydration is the introduction of phosphine ligands containing heterocyclic substituents. These allow for the formation of highly active and highly regioselective catalysts.[6-9] Ruthenium complexes of these self-assembled ligand systems have been applied in a wide range of catalytic reactions in recent years[12] including terminal alkyne hydration (Fig. 1).[10] Both the heterocycle-substituted phosphine ligand catalysts and self-assembled ligand catalysts are highly active and importantly highly selective for the formation of the *anti*-Markovnikov water addition product (an aldehyde). These systems are thought to utilise the both the metal centre and the functional groups present on the ligands in synergy during catalysis in an "enzyme-like" way.

This paper offers a combined experimental and computational mechanistic study of the catalytic hydration of terminal alkynes (using phenylacetylene as the alkyne model) by $[Ru(\eta^5\text{-}C_5H_5)(NCMe)(6\text{-}DPPAP)(3\text{-}DPICon)]PF_6$ (**1**), which has not been investigated in detail before. Additionally, experimental evidence of a non-productive catalyst deactivation pathway is presented, and a mechanism for the formation of the observed catalyst deactivation product has been proposed. The mechanistic features of related catalysts, based on imidazolyl and pyridyl phosphine ligands, have been investigated both experimentally and computationally in previous studies.[1, 6-9, 13] During the preparation of this manuscript a detailed computational study of the alkyne hydration mechanism in an imidazolyl phosphine system, which is highly relevant to the discussion here, was reported.[14] The key features of this study will be highlighted where appropriate in the discussion below.

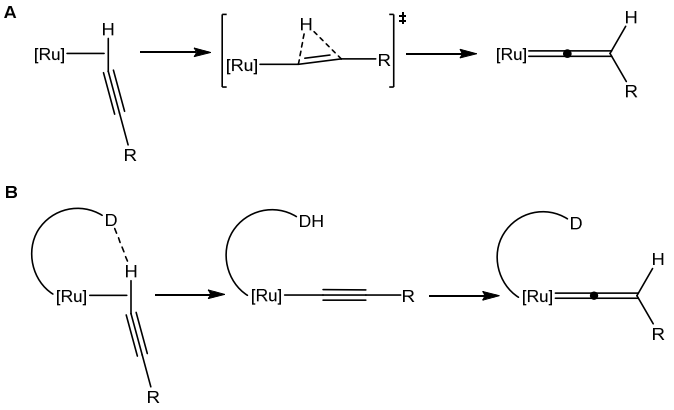

Figure 2: The two alkyne-vinylidene tautomerisation mechanisms considered here. **A**) Direct 1,2-hydrogen migration and **B**) A ligand-assisted proton shuttle (LAPS) mechanism; where D is a Lewis basic group close to the metal centre (e.g. the oxygen from a carboxylate ligand or basic nitrogen from the 6-DPPAP ligand).

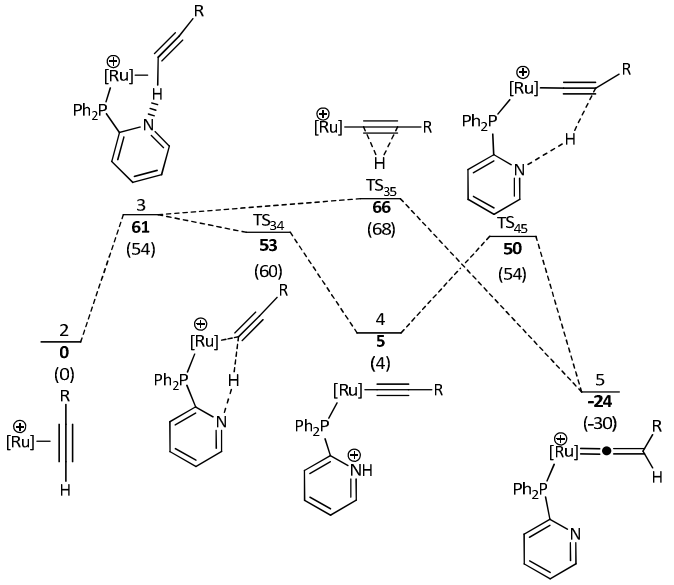

Figure 3: Potential energy surface for the formation of vinylidene complex **5** from the η^2-alkyne complex **2,** [Ru] = $[Ru(\eta^5\text{-}C_5H_5)(3\text{-}DPICon)(6\text{-}DPPAP)]$, R = Ph. Where appropriate, 6-DPPAP is partly shown. $E_{SCF+ZPE}$ (top, in bold) and relative Gibbs free energies at 298.15 K (bottom, in parentheses), both in acetone (COSMO solvation), are shown in kJ mol^{-1}.

Results and discussion

Computational studies

The reaction mechanism comprises a series of discrete stages; the first of which is the coordination of phenylacetylene to the metal in place of the labile MeCN ligand and subsequent alkyne-vinylidene tautomerisation. From the η^2-alkyne complex $[Ru(\eta^5\text{-}C_5H_5)(HCCPh)(6\text{-}DPPAP)(3\text{-}DPICon)]^+$ (**2**), the first step is slippage of the alkyne to allow coordination *via* the C-H σ-bond in **3** (see Figure 3). From **3**, two potential pathways can then be proposed. Like other electron-poor complexes, many ruthenium species undergo alkyne-vinylidene tautomerisation *via* a 1,2-hydrogen migration mechanism from the C-H σ-

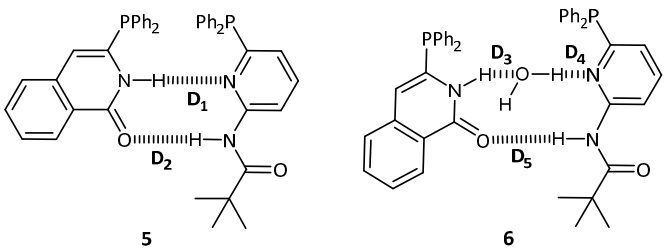

Hydrogen Bond	Length / Å
D1	1.87
D2	1.77
D3	1.68
D4	1.81
D5	1.81

Figure 4: Structures and hydrogen bond lengths in **5** and **6**. A hydrogen bond between the phosphines is retained during water incorporation (D_2 and D_5), maintaining the pseudo-bidentate nature of the ligand system. Ru and the other ligands are omitted for clarity.

complex directly to the vinylidene (Fig 2). However in this case, tautomerisation can also occur via a ligand-assisted proton shuttle (LAPS) mechanism,[4] which has been described recently in a ruthenium-acetate system. In this $[Ru(\kappa^2\text{-}OAc)_2(PPh_3)_2]$ reacts with phenylacetylene to form $[Ru(\kappa^1\text{-}OAc)(\kappa^2\text{-}OAc)(=C=CHPh)(PPh_3)_2]$ and the acetate ligand plays a key non-innocent role in the alkyne-vinylidene tautomerisation. In the case at hand the basic pyridyl-nitrogen atom of the aminopyridine moiety of 6-DPPAP can deprotonate the σ-complex **3** to form the acetylide **4**. The protonated 6-DPPAP ligand can then reprotonate the β-carbon of the acetylide to form vinylidene **5** (Fig. 2).

Figure 3 illustrates the potential energy surface (PES) for each of these processes. $E_{SCF+ZPE}$ energies in acetone solution will be used in the discussion below, as described in the experimental section. It can be noted that the energy barrier for the 1,2-hydrogen migration mechanism (*via* transition state **TS$_{35}$**) is 66 kJ mol^{-1}, whereas the barrier to the LAPS mechanism ($\Delta E_{SCF+ZPE}$ between **2** and **3**) is slightly lower at 61 kJ mol^{-1}. Although these barriers are very similar in energy at this level of theory, it does appear that ligand assistance from the 6-DPPAP ligand can facilitate both the deprotonation of the alkyne *via* **TS$_{34}$** and the reprotonation of the acetylide *via* **TS$_{45}$**. In the related $[Ru(\kappa^2\text{-}OAc)_2(PPh_3)_2]$ and $[Ru(\eta^5\text{-}C_5H_5)(PMe_2Im')_2]^+$ (where Im′ = 1,4-dimethylimidazol-2-yl) systems the LAPS mechanism involves Gibbs energies of activation of 32 and 86 kJ mol^{-1} respectively, suggesting that the nature of the ligands in these systems can play a significant role in the observed activation barriers.[4, 14]

A molecule of water can approach the vinylidene ligand in **5** and bind between one hydrogen bond of the phosphine ligands. In this way, the ligand set provides a water-binding pocket close to the metal centre that is important for catalysis (Fig 4). Binding of water into this pocket costs 26 kJ mol^{-1}, suggesting that the formation of hydrogen bonds D3 and D4 does not compensate for the loss of hydrogen bond D1 and the increased steric bulk around the metal centre. It should be noted that this process also involves a decrease in entropy that will disfavour

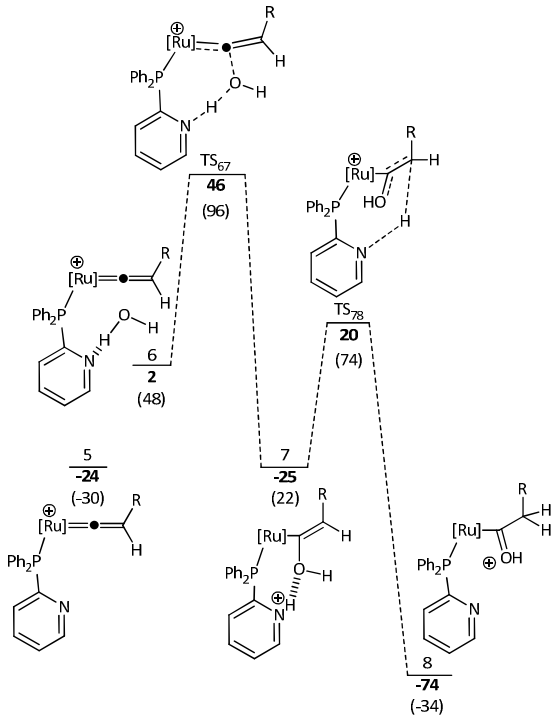

Figure 5: Potential energy surface for the formation of protonated acyl complex **8** from vinylidene complex **5,** [Ru] = $[Ru(\eta^5\text{-}C_5H_5)(3\text{-DPICon})]$, R = Ph, 6-DPPAP is partly shown. $E_{SCF+ZPE}$ (top, in bold) and relative Gibbs free energies at 298.15 K (bottom, in parentheses) in acetone (COSMO solvation) are shown in kJ mol^{-1}.

water binding, which is not included in the $E_{SCF+ZPE}$ energies (such entropy changes in solution are difficult to assess from gas phase calculations and so entropy corrections are not included here).[15]

The binding of water in between one hydrogen bond of the self-assembled ligand system without breaking of the other hydrogen bond shows the flexibility of these ligands in responding to the presence of substrates at ruthenium. This can also be seen in other states along the reaction coordinate. In almost all states during the LAPS processes described here (i.e. the formation of the vinylidene **5** from the alkyne **2**, the addition of water to the vinylidene and formation of the acyl **9** and protonation of the Ru-C bond to form the aldehyde product) only the first hydrogen bond (D_1 in Figure 4) is broken to facilitate the reaction. D_2 remains intact throughout these processes, except in complex **8**, where both hydrogen bonds are broken. Although D_1 is broken during these LAPS processes, the hydrogen bond donor and acceptor sites formerly involved in D_1 do become involved in hydrogen bonding to the O or OH groups of the substrate at various points along the reaction coordinate (in a similar way to what is seen on water binding in **6**).

The water-binding pocket within **6** both activates water such that it behaves as a better nucleophile, and holds it in close proximity with the correct orientation for attack at the α-carbon of the vinylidene ligand. The binding of water at a metal centre by heterocyclic ligands has also been observed experimentally in both imidazolyl and pyridyl phosphine complexes.[6, 7] The

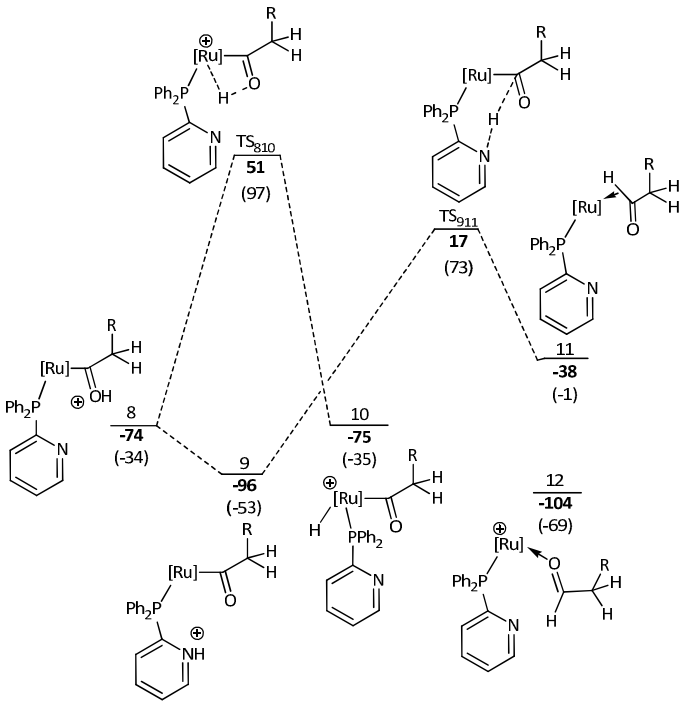

Figure **6**: Potential energy surface for the formation of complex **12** from protonated acyl complex **8,** [Ru] = [Ru(η^5-C_5H_5)(3-DPICon)], R = Ph, 6-DPPAP is partly shown. $E_{SCF+ZPE}$ (top, in bold) and relative Gibbs free energies at 298.15 K (bottom, in parentheses) in acetone (COSMO solvation) are shown in kJ mol^{-1}. The free aldehyde product and starting complex lie at **-142** (-104) kJ mol^{-1} relative to the reference point.

aminopyridine moiety of 6-DPPAP provides a basic site for the deprotonation of water as it attacks the vinylidene *via* $\mathbf{TS_{67}}$, with an energy barrier of 44 kJ mol^{-1} to form hydroxyvinyl species **7**. This complex is stabilised by a hydrogen bond between the protonated 6-DPPAP ligand and the oxygen atom of the hydroxyvinyl group. The N-H proton is then transferred to the β-carbon of the hydroxyvinyl group via $\mathbf{TS_{78}}$ to form complex **8** with an energy barrier of 45 kJ mol^{-1} (Fig. 5). These two steps represent a second LAPS process in the overall mechanism, where the basic nitrogen atom of the aminopyridine moiety again plays a key role as a proton shuttle.

Complex **8** can be formulated as either a protonated acyl or a hydroxycarbene. The metric parameters of the optimised structure of **8** suggest a contribution from both resonance forms, with an M-C bond length of 1.943 Å and a C-O distance of 1.335 Å. However, the calculations suggest that the reactivity of **8** may be dominated by the protonated acyl form. All attempts to locate a minimum energy structure where the O-H group points towards the basic nitrogen of the 6-DPPAP ligand to form a hydrogen bond resulted in proton transfer during the optimisation to form complex **9**. This suggests a low, or non-existent, barrier to this proton transfer that is consistent with a strongly Brønsted acidic O-H group.

From **8**, two possible pathways can be considered – the complex can undergo immediate deprotonation of the protonated acyl group by the basic nitrogen of 6-DPPAP and subsequent protonation of the α-carbon of the resulting acyl. Alternatively, **8** can isomerise to form a ruthenium (IV) hydride (this can be viewed as a protonation of Ru by the protonated acyl), which can form the aldehyde product by reductive elimination (Fig. 6). We were unable to find a transition state for proton transfer from the protonated acyl to 6-DPPAP. However, we expect this to be a low energy process, due to the high Brønsted acidity of the protonated acyl and high basicity of the aminopyridine group in 6-DPPAP.

Hydride formation costs 125 kJ mol^{-1} from **8**, but since the deprotonation of **8** to form **9** is thought to be a very low energy process, the formation of the hydride would actually have to proceed from **9**, resulting in a barrier of 147 kJ mol^{-1}. Unfortunately we were unable to locate a transition state for reductive elimination of the aldehyde product from **10** to form **11**. Protonation of the acyl carbon by the protonated 6-DPPAP ligand is also a high energy process, with a barrier of 113 kJ mol^{-1}, although this appears to be a more feasible pathway than formation of the hydride **10**. This high energy barrier can be rationalised by the formation of a very sterically hindered transition state and the protonation of the electron poor α-carbon of the acyl group. Again the 6-DPPAP ligand has acted as a proton shuttle, transferring a proton from oxygen to the β-carbon of the organometallic fragment in a third LAPS process during this mechanism.

Using the energetic span model of Kozuch and Shaik (where the TDI = **9** and the TDTS = $\mathbf{TS_{911}}$),[16] the energetic span for the formation of complex **11** is 113 kJ mol^{-1}. This is consistent with heating at a temperature of 120 °C for 26 hours being required during the catalytic reaction. The alternative mechanism, *via* the hydride **10**, has an energetic span of 147 kJ mol^{-1} (where the TDI = **9** and the TDTS is $\mathbf{TS_{810}}$), which reinforces the notion that the protonation of **9** *via* $\mathbf{TS_{911}}$ is a more likely pathway. A related DFT study by Cooksy on Grotjahn's [Ru[(η^5-C_5H_5)(PMe_2Im')$_2$]$^+$ (where Im′ = 1,4-dimethylimidazol-2-yl) based alkyne hydration catalysts finds that the energetic span for this system is also 113 kJ mol^{-1} (where the TDI = is the Ru-OH_2 starting complex and the TDTS = deprotonation of the Ru-alkyne complex by the basic nitrogen atom of an imidazolyl moiety to form a ruthenium-acetylide).[14] The identification of the turnover-determining states in this system assumes, as noted by Cooksy, that the initial water-alkyne exchange reaction, which has a high barrier in these calculations, is unlikely to be well modelled and as such that the transition state for this step is not likely to be the TDTS.

It is interesting to note that the turnover-determining states are rather different in the two systems. In the 6-DPPAP/3-DPICon system alkyne deprotonation is facile, but protonation of the ruthenium-carbon bond of the acyl to release the aldehyde is a high-energy process. In the imidazolyl phosphine system, deprotonation of the alkyne is a high-energy process, perhaps due to the formation of two hydrogen bonds between the alkyne protons of the acetylene ligand used in the study that must be broken in order to rearrange the system to form the alkyne-deprotonation transition state. However, protonation of the ruthenium-carbon bond of the acyl complex is more

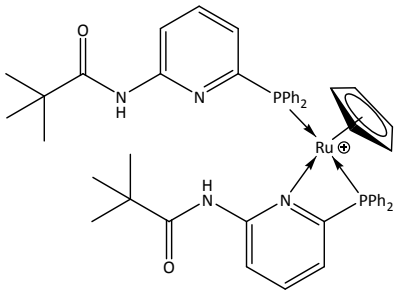

Figure 7: Proposed structure of $[(\eta^5\text{-}C_5H_5)Ru(6\text{-}DPPAP)_2][PF_6]$ (**13**)

favourable than in the 6-DPPAP/3-DPICon system. These subtle ligand effects suggest that careful tuning of these functionalised ligand systems is likely to be a useful design strategy for reaction optimisation.

Experimental studies

The mechanism of alkyne hydration catalysed by **1** was also investigated using stoichiometric experimental studies, in an attempt to observe possible intermediates in the process. Preparation of $[Ru(\eta^5\text{-}C_5H_5)(NCMe)(6\text{-}DPPAP)(3\text{-}DPICon)]PF_6$, **1**, required some care. Addition of 6-DPPAP and 3-DPICon simultaneously to $[Ru(\eta^5\text{-}C_5H_5)(NCMe)_3]PF_6$ in acetone, chloroform or dichloromethane yielded a mixture of organometallic species. Independent syntheses confirmed these to be $[Ru(\eta^5\text{-}C_5H_5)(6\text{-}DPPAP)_2]PF_6$ (**13**) and $[Ru(\eta^5\text{-}C_5H_5)(NCMe)(3\text{-}DPICon)_2]PF_6$ (**14**), which appeared as a doublet at -16.5 ppm ($^2J_{PP}$ = 38.2 Hz) and a singlet at 50.4 ppm respectively in the $^{31}P\{^1H\}$ NMR spectra.

The chemical shift of the doublet at -16.5 ppm for **13** is significantly upfield compared to related ruthenium-phosphine complexes of this type, and was indicative of a chelating binding mode for one 6-DPAAP ligand; where both phosphorus and the nitrogen atom of the aminopyridine motif in one 6-DPPAP ligand both coordinate to the metal (Fig. 7). Similar binding of pyridyl- and imidazolyl phosphine ligands has been reported in the literature by Grotjahn and others.[1, 17] Heating mixtures of **13** and **14** synthesised *via* this route did not affect the organometallic product distribution, but introduced additional signals in the $^{31}P\{^1H\}$ NMR spectra, presumably due to degradation. A pure sample of **1** was obtained through dissolution of $[Ru(\eta^5\text{-}C_5H_5)(NCMe)_3]PF_6$ in dichloromethane and stoichiometric addition of one equivalent of 3-DPICon, followed by subsequent addition of one equivalent of 6-DPPAP. The analytical data for **1** synthesised by this method matches that in the literature; the $^{31}P\{^1H\}$ NMR spectrum shows two doublets at 54.2 and 49.0 ($^2J_{PP}$ = 36.5 Hz).[10]

On addition of an alkyne to **1**, formation of the acetylide **4** or vinylidene **5** (see Figure 3) was anticipated, as DFT studies showed these to be minima with moderate energy barriers to formation. However, no reaction was observed between **1** and a range of alkynes (1-nonyne, phenylacetylene, 4-ethynyl-α,α,α-trifluorotoluene) at room temperature after stirring for 24 hours in dichloromethane. This may be due to a larger barrier for MeCN/alkyne exchange than alkyne-vinylidene

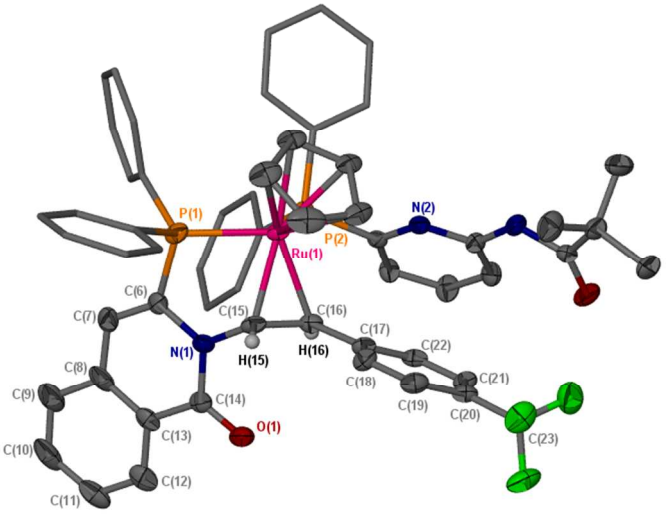

Figure 8: Crystal structure of complex **15**. Thermal ellipsoids (where shown) at the 50% probability level, hydrogen atoms (except H_{15} and H_{16}), a dichloromethane and diethyl ether of crystallisation and the PF_6 counter-ion are omitted for clarity. Selected bond lengths (Å) and angles (°) C(15)-C(16) 1.405(6), C(15)-N(1) 1.469(6), Ru(1)-C(15) 2.181(4), Ru(1)-C(16) 2.248(4), P(1)-C(6)-N(1) 109.1(3), C(6)-N(1)-C(15) 118.7(4), N(1)-C(15)-C(16) 119.0(4), C(15)-C(16)-C(17) 123.0(4).

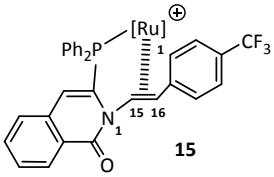

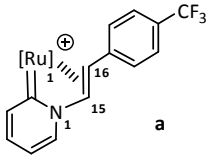

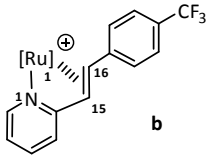

	Structure			
		15	**a**	**b**
Bond Lengths/ Å	C(15)-C(16)	1.405(6)	1.406(4)	1.404(4)
	N(1)-C(15)	1.469(6)	1.459(4)	-
	Ru(1)-C(15)	2.181(4)	2.127(3)	2.188(3)
	Ru(1)-C(16)	2.248(4)	2.245(3)	2.274(3)

Figure 9: Comparison of single-crystal X-ray crystallography data in a series of related ruthenium complexes.[20]

tautomerisation, which prevents alkyne binding under these conditions. The reverse reaction relating to this process has been studied in some detail in a related system.[18] This ligand exchange process has not been modelled in this study due to the difficulty in accurately assessing the energetics of this process (most notably the role of solvent and entropic effects). Upon heating a mixture of **1** and phenylacetylene at 50 °C in dichloromethane, highly selective conversion to a new organometallic species was observed. The $^{31}P\{^1H\}$ NMR spectrum of this product showed the emergence of two new resonances (δ 65.4, d, $^2J_{PP}$ = 32.4 Hz and δ 40.3, br). The ^1H NMR spectrum indicated that the hydrogen bonding network

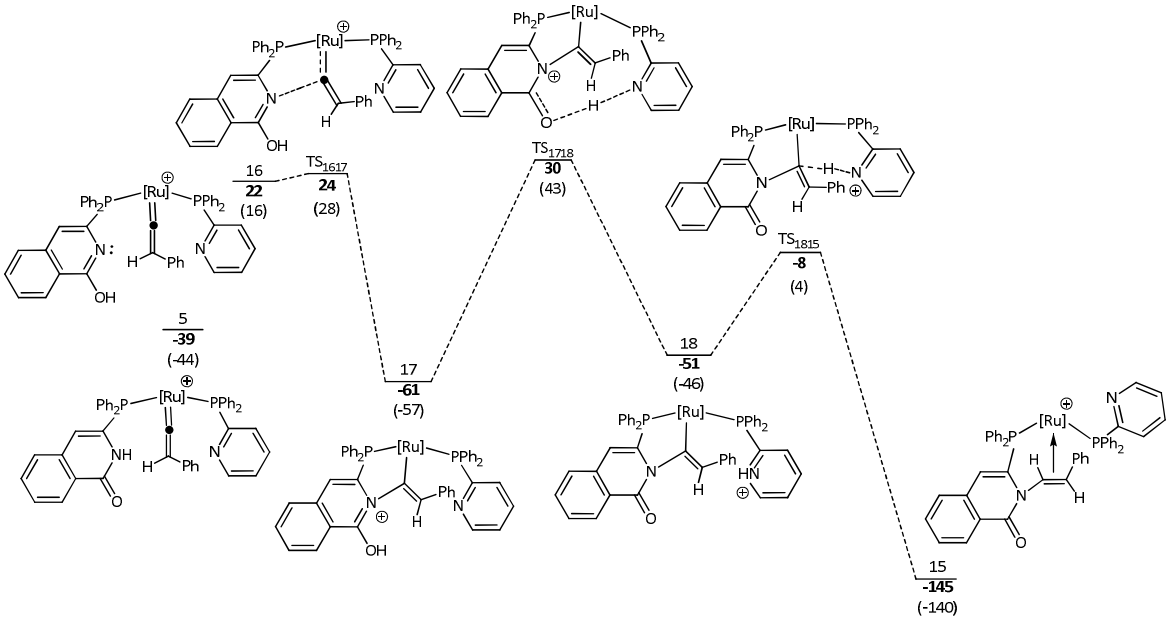

Figure 10: Potential energy surface for the formation of complex **15** from vinylidene **5**, [Ru] = [Ru(η^5-C_5H_5)], 6-DPPAP is partly shown. Relative $E_{SCF+ZPE}$ (top, in bold) and Gibbs free energy at 298.15 K (bottom, in parentheses) in dichloromethane (COSMO solvation) are shown in kJ mol^{-1}.

present in **1**, characterised by very downfield signals for the two N-H protons, had been lost during the reaction.

However, the expected vinylidene **5** was not observed. This was confirmed by the reaction of **1** with ^{13}C-labelled phenylacetylene, as no signal for the vinylidene carbon was observed in the ^{13}C NMR spectra (expected at approximately δ 350).[19] Curiously though, high-resolution mass spectrometry (ESI ionisation) showed an organometallic species with the exact mass of the expected vinylidene complex. A single-crystal X-ray structure of an analogous reaction of **1** with 4-ethynyl-α,α,α-trifluorotoluene confirmed this to be complex **15** (Fig. 8), the formation of which occurs from a formal insertion of the alkyne into the N-H bond of the isoquinolone moiety of 3-DPICon.

The structure of **15** shows notable differences to **1**, the parent complex from which it is derived. Alkyne insertion into the 3-DPICon ligand causes loss of the hydrogen bonding network between 3-DPICon and 6-DPPAP and increased steric bulk around the ruthenium centre, which leads to structural changes both in terms of conformation and bond lengths. The pyridyl-nitrogen of the 6-DPPAP ligand cannot engage in hydrogen bonding with the amide moiety of 3-DPICon, and so orients towards the cyclopentadienyl ligand to minimise steric congestion. Differences are also observed in the bond lengths of the 3-DPICon isoquinolone moiety; lengthening of the C(14)-N(1) bond and a contraction of C(14)-O(1) is consistent with the loss of the hydrogen bonding network.

Complex **15** also shows remarkable similarities to a related ruthenium pyridylidene complex we have previously reported (Complex **a**, Fig 9).[20] Although it must be noted that **15** is based on a pyridyl phosphine rather than a pyridylidene backbone, very similar bond lengths are observed between N(1)-C(15), C(15)-C(16) and between Ru(1)-C(15). The notably longer Ru(1)-C(15) bond length may be due to the difference in ring size between the two structures. An isomer of **a** has also been studied by single-crystal x-ray crystallography, (complex **b**, Fig. 9). The bond lengths indicate that the binding of the alkene is similar for all of these examples of ruthenium d^6 complexes. Complex **15** was investigated for catalytic activity, but under normal catalytic conditions[†] no aldehyde formation was observed.

A potential mechanism for the formation of **15** (using CH_2Cl_2 COSMO solvation to mirror the experimental studies) is shown in Fig. 10. The proposed reaction pathway comprises a number of stages, and the vinylidene complex **5** can be considered a branching point for the productive and non-productive catalyst pathways. From **5**, lactam-lactim tautomerism of the isoquinolone moiety in 3-DPICon reveals the nucleophilic nitrogen atom of a hydroxyisoquinoline motif (**16**). Attack of this nitrogen atom at the α-carbon of the vinylidene *via* $\mathbf{TS_{1617}}$ leads to a 5-membered metallocycle (**17**). Intramolecular proton transfer between the two phosphine ligands in **17** then returns the 3-DPICon ligand to its isoquinolone-containing tautomer (**18**). A final proton transfer from the N-H group of the 6-DPPAP ligand to the α-carbon of the metallocycle yields the final organometallic species **15**. Thus, the Lewis basic nitrogen atom of 6-DPPAP is involved in yet another LAPS process, in this case shuttling a proton from the 3-DPICon ligand to the alkyne. The largest energy barrier for this process is 91 kJ mol^{-1}, which corresponds to the intramolecular proton transfer between the ligands. We were unable to locate a transition state for isomerisation of 3-DPICon to its hydroxyisoquinoline-containing tautomer. However, this type of lactam-lactim tautomerism is well known and could occur *via* an intramolecular, intermolecular or solvent-mediated mechanism.

Using the energetic span model of Kozuch and Shaik (where the TDI = **17** and the TDTS = $\mathbf{TS_{1718}}$), the energetic span for the formation of **15** in CH_2Cl_2 is quite modest at 91 kJ mol^{-1}, which is consistent with the observation of this product after heating at 50 °C in CH_2Cl_2 over several days. When compared to the productive catalytic pathway, which has an energetic span of 113 kJ mol^{-1} in acetone, it seems that **15** is a kinetic product in this system. **15** is also rather stable compared to other states (at -145 kJ mol^{-1}). Indeed it is similarly stable to formation of the aldehyde product during the productive catalyst pathway (-142 kJ mol^{-1}). The stability of **15** results in the back reaction to form the vinylidene **5**, from which productive catalysis could occur, being a high energy process. The energetic span for formation of the aldehyde product from **15** is large at 175 kJ mol^{-1} (where the TDI = **15** and the TDTS = $\mathbf{TS_{1718}}$). Experimental studies confirm that **15** is not an active catalyst under the normal catalytic conditions and it can therefore be considered a catalyst deactivation product. There are similarities between this catalyst deactivation mechanism and one which we have reported recently in a related pyridine alkenylation catalyst.[20]

Although one might expect to see quite rapid deactivation of the catalyst under normal operating conditions, based on the smaller energetic span for the formation of **15** compared to the productive pathway, in fact this is not the case. Although a significant amount of **15** is observed in the $^{31}P\{^1H\}$ NMR spectrum (40.3 (br), 65.5 (d, $^2J_{PP}$ = 32.4 Hz)) of the reaction mixture following a catalytic run,[†] the rate of deactivation appears to be slow enough not to prevent productive catalysis. It should be noted that the catalyst deactivation described above occurs under somewhat different conditions to the active catalytic conditions (CH_2Cl_2 as solvent compared to acetone, at lower temperature and in the absence of water). Although when the energetic span of the deactivation reaction is calculated with acetone solvation (see ESI for details) it is the same as in CH_2Cl_2 (91 kJ mol^{-1}) and so implicit solvation does not help us to understand the differences here. Our investigations have not been able to determine the origin of this effect, but it may be that under active catalytic conditions the binding of water to the 3-DPICon and/or 6-DPPAP ligands at one or more points along the reaction coordinate inhibits the deactivation pathway sufficiently to allow productive catalysis.

Conclusions

On the basis of a thorough mechanistic study using DFT, and supported by experimental evidence from similar systems and a recent computational study on a related catalyst, we have proposed a catalytic pathway for the hydration of terminal alkynes by the self-assembled phosphine complex $[Ru(\eta^5\text{-}C_5H_5)(NCMe)(6\text{-}DPPAP)(3\text{-}DPICon)]PF_6$, **1**. Catalysis is thought to involve three ligand-assisted proton shuttle (LAPS) processes (during vinylidene formation, water addition to the vinylidene and tautomerisation from a hydroxyvinyl to acyl complex) that are enabled by the functionality present in the phosphine ligands. In this way the ligands play as important a role in the catalytic mechanism as the metal centre and this system can therefore be compared to some metalloenzymes where the metal centre and protein backbone both play a role in catalysis. The experimental study has highlighted a new catalyst deactivation product, **15**, in this system and mechanism has been suggested for the formation of this product. This involves yet another example of a LAPS process mediated by the self-assembled ligand system and involves initial lactam-lactim tautomerism of the isoquinolone moiety of the 3-DPICon ligand. **15** is a kinetic (and potentially also the thermodynamic) product in this system (in CH_2Cl_2) and represents a catalyst deactivation pathway, as the energetic span for productive catalysis from **15** is large. Experiments have confirmed that **15** is not an active catalyst.

Experimental

General methods

Calculations were performed at the (RI-)PBE0/def2-TZVPP//(RI-)BP86/SV(P) level (a methodology that we have validated in a related system)[21] with the full ligand substituents used in the experimental study (Fig. 1) using TURBOMOLE.[22] Data presented on the potential energy surfaces (PES) includes acetone solvation for the catalytic reaction, and dichloromethane solvation for the stoichiometric studies (using the COSMO method).[23] Single-point DFT-D3 corrections (on the (RI)-BP86/SV(P) geometries) have been applied at the PBE0-D3 level using Grimme's DFT-D3 (V3.0 Rev 2, with with BJ-damping) program and data presented on the PESs includes this correction.[24] Gas-phase data is provided in the supplementary information. Both ZPE-corrected SCF energies ($E_{SCF+ZPE}$) and Gibbs energies at 298.15 K are shown on the PES and energies quoted are relative to alkyne complex **2** + water + MeCN. $E_{SCF+ZPE}$ data are discussed in the main section of the manuscript due to the difficulty in assessing entropy changes in solution from gas-phase calculations.[15] Dotted lines on the PESs indicate connectivity between minima and transition states. Minima were confirmed as such by the absence of imaginary frequencies, and transition states were identified by the presence of one imaginary frequency with subsequent verification by DRC analyses. In cases where it was not possible to locate a transition state, connections to neighbouring states *via* dotted lines are not shown.

All air-sensitive experimental procedures were performed under an inert atmosphere of nitrogen using standard Schlenk line and glovebox techniques. Dichloromethane and pentane were purified with the aid of an Innovative Technologies anhydrous solvent engineering system. Acetone was degassed by bubbling with N_2 before use. The CD_2Cl_2 used for NMR experiments was dried over CaH_2 and degassed with three freeze-pump-thaw cycles. The solvent was then transferred into NMR tubes fitted with PTFE Young's taps or stored under a nitrogen atmosphere in the Glove Box. NMR spectra were acquired on a Jeol ECX-400 (Operating frequencies ^1H 399.78 MHz, ^{31}P 161.83 MHz, ^{19}F 376.17 MHz, ^{13}C 100.53 MHz),

aBruker AVANCE 500 (Operating frequencies ^{1}H 500.13 MHz, ^{31}P 202.47 MHz, ^{13}C 125.77 MHz) or a Bruker AVANCE 700 (Operating frequencies ^{1}H 700.13 MHz, ^{31}P 283.46 MHz, ^{13}C 176.07 MHz). ^{31}P and ^{13}C spectra were recorded with proton decoupling. Assignments were confirmed with the aid of 2D-COSY, NOESY, HMQC and HMBC experiments. Mass spectra were recorded on a Bruker micrOTOF using electrospray ionisation.

Synthesis and spectroscopic data for 15

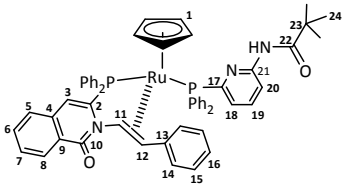

To a Young's NMR tube was added [Ru(η^5-C_5H_5)(NCMe)$_3$]PF_6 (20 mg, 46 µmol) and 3-DPICon (15 mg, 46 µmol, 1 equivalent) in deuterated dichloromethane (0.5 ml). After two hours, 6-DPPAP was added (16 mg, 46 µmol, 1 equivalent) and the reaction was heated at 50 °C for 20 hours (until [Ru(η^5-C_5H_5)(6-DPPAP)(3-DPICon)]PF_6 was the only product in the ^{31}P{^{1}H} NMR spectrum). Phenylacetylene was added (6.3 µl, 138 µmol, 3 equivalents) and the reaction heated at 50 °C for 1 week.

^{1}H NMR (CD_2Cl_2, 400 MHz, 295 K): δ 1.20 (s, 9H, H_{24}), 5.00 (s, 5H, H_1), 6.00 (br, 1H), 6.32 (br, 2H), 6.48 (d, *J* = 6.7 Hz, 1H), 6.53 (dd, *J* = 7.4, 3.5 Hz, 1H), 6.65 (br, 2H), 6.97 (dd, *J* = 9.9, 3.2 Hz, 1H, H_{12}), 7.00 – 7.10 (m, 4H), 7.21 (m, 4H), 7.27 – 7.40 (m, 4H), 7.43 – 7.46 (d, *J* = 7.9 Hz, 1H), 7.46 – 7.50 (m, 3H), 7.50 – 7.55 (m, 2H), 7.55 – 7.61 (m, 3H), 7.64 – 7.80 (m, 6H), 8.31 (d, *J* = 7.8 Hz, 1H), 8.39 (d, *J* = 7.1 Hz, 1H). ^{13}C NMR (CD_2Cl_2, 100 MHz, 295 K): δ 27.4 (s, C_{24}), 40.0 (s, C_{23}), 62.3 (s, C_{11}), 76.4 (d, *J* = 6.7 Hz, C_{12}), 93.2 (s, C_1), 110.9 (d, *J* = 2.9 Hz), 116.1 (s), 124.6 (d, *J* = 14.5 Hz), 126.0 (s), 127.5 (s), 128.1 (d, *J* = 8.0 Hz), 128.8 (d, *J* = 9.2 Hz), 129.1 (d, *J* = 10.2 Hz), 129.2 (d, *J* = 6.8 Hz), 130.1 (d, *J* = 10.9 Hz), 130.3 (d, *J* = 10.9 Hz), 131.3 (d, *J* = 2.2 Hz), 131.9 (d, *J* = 2.6 Hz), 132.3 (d, *J* = 2.3 Hz), 132.5 (s), 132.6 (d, *J* = 10.6 Hz), 133.2 (d, *J* = 11.5 Hz). 133.6 (d, *J* = 9.2 Hz), 133.7 (s), 134.4 (d, *J* = 19.6 Hz), 137.0 (d, *J* = 9.1 Hz), 139.7 (d, *J* = 5.9 Hz), 141.3 (s), 143.8 (d, *J* = 66.3 Hz), 153.5 (d, *J* = 18.9 Hz), 156.1 (d, *J* = 72.3 Hz, $C_{2/17}$), 163.9 (d, *J* = 9.9 Hz, C_{10}), 177.1 (s, C_{22}). Residual resonances for free phenylacetylene and acetonitrile have been omitted. ^{31}P NMR (CD_2Cl_2, 162 MHz, 295 K): δ -143.0 (sept, $^{1}J_{PF}$ = 711 Hz, PF_6^-), 40.3 (br), 65.5 (d, $^{2}J_{PP}$ = 32.4 Hz). MS (ESI+): Measured m/z = 960.2372, $[M]^+$, calculated m/z for $C_{56}H_{50}N_3O_2P_2Ru^+$ = 960.2431 (Δ = 4.4 mDa)

Synthesis and spectroscopic data for 15^{CF3}

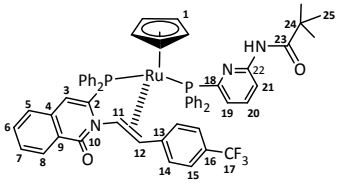

To a Young's NMR tube was added [Ru(η^5-C_5H_5)(NCMe)$_3$]PF_6 (20 mg, 46 µmol) and 3-DPICon (15 mg, 46 µmol, 1 equivalent) in deuterated dichloromethane (0.5 ml). After two hours, 6-DPPAP was added (16 mg, 46 µmol, 1 equivalent) and the reaction heated at 50 °C for 20 hours (until [Ru(η^5-C_5H_5)(6-DPPAP)(3-DPICon)]PF_6 was the only product in the ^{31}P NMR). 4-ethynyl-α,α,α-trifluorotoluene was added (9.3 µl, 138 µmol, 3 equivalents) and the reaction heated at 50 °C for 1 week.

^{1}H NMR (CD_2Cl_2, 700 MHz, 290 K): δ 1.17 (s, 9H, H_{25}), 4.73 (br, 1H, H_{11}), 5.05 (s, 5H, H_1), 5.96 (br, 1H), 6.25 (br, 2H), 6.47 (d, *J* = 6.7 Hz, 1H), 6.52 (br, 1H), 6.56 – 6.71 (br, 2H), 6.93 (br, d, *J* = 8.4 Hz, 1H, H_{12}), 6.96 – 7.12 (m, 4H), 7.18 – 7.32 (m, 3H), 7.44 (d, J = 7.7 Hz, 2H), 7.48 – 7.53 (br, 3H), 7.57 – 7.58 (m, 1H), 7.59 – 7.64 (m, 10H), 7.66 (br, 1H), 7.69 – 7.78 (m, 5H), 8.29 (d, *J* = 7.8 Hz, 1H), 8.38 (d, *J* = 6.6 Hz, 1H). ^{13}C NMR (176 MHz, 290 K): δ 26.9 (s, C_{25}), 39.6 (s, C_{24}), 58.5 (s, C_{11}), 76.4 (d, 5.9 Hz, C_{12}), 87.6 (s), 93.0 (s, C_1), 110.8 (s), 116.0 (s), 123.9 (q, $^{1}J_{CF}$ = 271 Hz, C_{17}), 124.4 (d, *J* = 14.4 Hz), 125.2 (q, $^{3}J_{CF}$ = 3.8 Hz, C_{15}), 125.5 (s, quat.), 125.9 (br, quat.), 127.2 (s), 127.7 (s), 128.5 (d, *J* = 9.2 Hz), 128.8 (d, *J* = 10.8 Hz), 129.2 (s), 129.8 (d, *J* = 11.2 Hz), 130.0 (d, *J* = 10.7 Hz), 130.3 (q, $^{2}J_{CF}$ = 32.6 Hz, C_{16}), 131.1 (s), 131.7 (s), 131.9 (br, quat.), 132.0 (br), 132.3 (d, *J* = 10.2 Hz), 132.5 (s), 132.8 (br), 133.2 (br), 133.5 (s), 136.6 (d, *J* = 8.6 Hz, quat.), 139.4 (br), 143.3 (d, *J* = 67.6 Hz, $C_{2/18}$), 145.8 (s, C_{22}), 155.9 (d, *J* = 71.2 Hz, $C_{2/18}$), 163.4 (d, *J* = 9.8 Hz, C_{10}), 176.8 (s, C_{23}). Residual resonances for free alkyne and acetonitrile have been omitted. ^{31}P NMR (CD_2Cl_2, 162 MHz, 295 K): δ -143.0 (sept, $^{1}J_{PF}$ = 711 Hz, PF_6^-), 39.5 (br), 65.1 (d, $^{2}J_{PP}$ = 31.4 Hz). ^{19}F NMR (CD_2Cl_2, 376 MHz, 295 K): δ -72.7 (PF_6^-), -63.2 (CF_3). MS (ESI+): Measured m/z = 1028.2245, $[M]^+$, calculated m/z for $C_{57}H_{49}F_3N_3O_2P_2Ru^+$ = 1028.2305 (Δ = 4.5 mDa)

Acknowledgements

We thank the Alexander von Humboldt foundation, the EPSRC (Grants GR/H011455/1 and EP/K031589/1) and the University of York for funding. JMS is very grateful to Prof. Ingo Krossing for help and advice and for providing access to the computational hardware required to initiate this project, which ignited his interest in mechanistic organometallic chemistry some years ago.

Notes and references

[a] Department of Chemistry, University of York, Heslington, York, YO10 5DD Fax: +44(0)1904322516; Tel: +44(0)1904322610; E-mail: john.slattery@york.ac.uk, jason.lynam@york.ac.uk

[b] Institut für Organische Chemie & Biochemie, Albert-Ludwigs-Universität Freiburg, Albertstr. 21a, 79104 Freiburg i. Brsg., Germany.

† Catalytic Conditions: 2 mol % **1**, 1 mmol alkyne and 5 mmol water in 1.6ml deoxygenated acetone. Reaction was heated under N_2 for 26 hours in a sealed tube at 120 °C.

Electronic Supplementary Information (ESI) available: incudes SCF energies, ZPEs, XYZ coordinates and vibrational frequencies for all

stationary points. Full experimental details are also given in the ESI. See DOI: 10.1039/b000000x/

1. D. B. Grotjahn, *Chem. Eur. J.*, 2005, **11**, 7146-7153.
2. D. Lapointe and K. Fagnou, *Chem. Lett.*, 2010, **39**, 1119-1126.
3. Y. Boutadla, D. L. Davies, S. A. Macgregor and A. I. Poblador-Bahamonde, *Dalton Trans.*, 2009, 5820-5831; Y. Boutadla, D. L. Davies, S. A. Macgregor and A. I. Poblador-Bahamonde, *Dalton Trans.*, 2009, 5887-5893; D. L. Davies, S. M. A. Donald, O. Al-Duaij, J. Fawcett, C. Little and S. A. Macgregor, *Organometallics*, 2006, **25**, 5976-5978; D. L. Davies, S. M. A. Donald, O. Al-Duaij, S. A. Macgregor and M. Polleth, *J. Am. Chem. Soc.*, 2006, **128**, 4210-4211; D. L. Davies, S. M. A. Donald and S. A. Macgregor, *J. Am. Chem. Soc.*, 2005, **127**, 13754-13755; D. L. Davies, S. A. Macgregor and A. I. Poblador-Bahamonde, *Dalton Trans.*, 2010, **39**, 10520-10527.
4. D. G. Johnson, J. M. Lynam, J. M. Slattery and C. E. Welby, *Dalton Trans.*, 2010, **39**, 10432–10441.
5. J. Guihaume, S. Halbert, O. Eisenstein and R. N. Perutz, *Organometallics*, 2012, **31**, 1300-1314.
6. D. B. Grotjahn, C. D. Incarvito and A. L. Rheingold, *Angew. Chem., Int. Ed.*, 2001, **40**, 3884-3887.
7. D. B. Grotjahn, E. J. Kragulj, C. D. Zeinalipour-Yazdi, V. Miranda-Soto, D. A. Lev and A. L. Cooksy, *J. Am. Chem. Soc.*, 2008, **130**, 10860-10861.
8. D. B. Grotjahn and D. A. Lev, *J. Am. Chem. Soc.*, 2004, **126**, 12232-12233.
9. D. B. Grotjahn and D. A. Lev, *Chem. Indust.*, 2005, **104**, 227-236.
10. F. Chevallier and B. Breit, *Angew. Chem. Int. Ed.*, 2006, **45**, 1599 – 1602.
11. M. Tokunaga and Y. Wakatsuki, *Angew. Chem., Int. Ed.*, 1998, **37**, 2867-2869; M. Tokunaga, T. Suzuki, N. Koga, T. Fukushima, A. Horiuchi and Y. Wakatsuki, *J. Am. Chem. Soc.*, 2001, **123**, 11917-11924.
12. V. Agabekov, W. Seiche and B. Breit, *Chem. Sci.*, 2013, **4**, 2418-2422; M. N. Birkholz, N. V. Dubrovina, H. J. Jiao, D. Michalik, J. Holz, R. Paciello, B. Breit and A. Borner, *Chem. Eur. J.*, 2007, **13**, 5896-5907; B. Breit, *Angew. Chem., Int. Ed.*, 2005, **44**, 6816-6825; B. Breit, *Pure Appl. Chem.*, 2008, **80**, 855-860; B. Breit, *Abstr. Pap. Am. Chem. Soc.*, 2013, **245**; B. Breit and W. Seiche, *J. Am. Chem. Soc.*, 2003, **125**, 6608-6609; B. Breit and W. Seiche, *Angew. Chem., Int. Ed.*, 2005, **44**, 1640-1643; B. Breit and W. Seiche, *Pure Appl. Chem.*, 2006, **78**, 249-256; M. de Greef and B. Breit, *Angew. Chem., Int. Ed.*, 2009, **48**, 551-554; L. Diab, U. Gellrich and B. Breit, *Chem. Commun.*, 2013, **49**, 9737-9739; L. Diab, T. Smejkal, J. Geier and B. Breit, *Angew. Chem., Int. Ed.*, 2009, **48**, 8022-8026; D. Fuchs, G. Rousseau, L. Diab, U. Gellrich and B. Breit, *Angew. Chem., Int. Ed.*, 2012, **51**, 2178-2182; U. Gellrich, J. Huang, W. Seiche, M. Keller, M. Meuwly and B. Breit, *J. Am. Chem. Soc.*, 2011, **133**, 964-975; U. Gellrich, W. Seiche, M. Keller and B. Breit, *Angew. Chem., Int. Ed.*, 2012, **51**, 11033-11038; A. C. Laungani and B. Breit, *Chem. Commun.*, 2008, 844-846; A. C. Laungani, M. Keller, J. M. Slattery, I. Krossing and B. Breit, *Chem. Eur. J.*, 2009, **15**, 10405-10422; A. C. Laungani, J. M. Slattery, I. Krossing and B. Breit, *Chem. Eur. J.*, 2008, **14**, 4488-4502; W. Seiche, A. Schuschkowski and B. Breit, *Adv. Synth. Catal.*, 2005, **347**, 1488-1494; T. Smejkal and B. Breit, *Organometallics*, 2007, **26**, 2461-2464; T. Smejkal and B. Breit, *Angew. Chem., Int. Ed.*, 2008, **47**, 311-315; T. Smejkal and B. Breit, *Angew. Chem., Int. Ed.*, 2008, **47**, 3946-3949; A. T. Straub, M. Otto, I. Usui and B. Breit, *Adv. Synth. Catal.*, 2013, **355**, 2071-2075; L. Usui, S. Schmidt, M. Keller and B. Breit, *Org. Lett.*, 2008, **10**, 1207-1210; C. Waloch, J. Wieland, M. Keller and B. Breit, *Angew. Chem., Int. Ed.*, 2007, **46**, 3037-3039; M. Weis, C. Waloch, W. Seiche and B. Breit, *J. Am. Chem. Soc.*, 2006, **128**, 4188-4189; J. Wieland and B. Breit, *Nature Chem.*, 2010, **2**, 832-837.
13. A. Labonne, T. Kribber and L. Hintermann, *Org. Lett.*, 2006, **8**, 5853-5856; T. Kribber, A. Labonne and L. Hintermann, *Synthesis-Stuttgart*, 2007, 2809-2818.
14. A. J. Arita, J. Cantada, D. B. Grotjahn and A. L. Cooksy, *Organometallics*, 2013, **32**, 6867-6870.
15. B. O. Leung, D. L. Reid, D. A. Armstrong and A. Rauk, *J. Phys. Chem. A*, 2004, **108**, 2720-2725; D. Ardura, R. López and T. L. Sordo, *J. Phys. Chem. B.*, 2005, **109**, 23618-23623; P. A. Dub and R. Poli, *J. Mol. Cat. A*, 2010, **324**, 89-96.
16. S. Kozuch and S. Shaik, *Acc. Chem. Res.*, 2010, **44**, 101-110.
17. K. Q. A. Lenero, Y. Guari, P. C. J. Kamer, P. W. N. M. van Leeuwen, B. Donnadieu, S. Sabo-Etienne, B. Chaudret, M. Lutz and A. L. Spek, *Dalton Trans.*, 2013, **42**, 6495-6512.
18. M. Bassetti, V. Cadierno, J. Gimeno and C. Pasquini, *Organometallics*, 2008, **27**, 5009-5016.
19. M. I. Bruce, *Chem. Rev.*, 1991, **91**, 197-257; M. J. Cowley, J. M. Lynam, R. S. Moneypenny, A. C. Whitwood and A. J. Wilson, *Dalton Trans.*, 2009, 9529-9542; C. E. Welby, T. O. Eschemann, C. A. Unsworth, E. J. Smith, R. J. Thatcher, A. C. Whitwood and J. M. Lynam, *Eur. J. Inorg. Chem.*, 2012, 1493-1506.
20. D. G. Johnson, J. M. Lynam, N. S. Mistry, J. M. Slattery, R. J. Thatcher and A. C. Whitwood, *J. Am. Chem. Soc.*, 2013, **135**, 2222-2234; J. M. Lynam, L. M. Milner, N. S. Mistry, J. M. Slattery, S. R. Warrington and A. C. Whitwood, *Dalton Trans.*, 2014, **43**, 4565-4572.
21. M. J. Cowley, J. M. Lynam and J. M. Slattery, *Dalton Trans.*, 2008, 4552-4554.
22. R. Ahlrichs, M. Baer, M. Haeser, H. Horn and C. Koelmel, *Chem. Phys. Lett.*, 1989, **162**, 165; M. v. Arnim and A. R., *J. Chem. Phys.*, 1999, **111**, 9183-9190; P. Császár and P. Pulay, *J. Mol. Str.*, 1984, **114**, 31-34; P. Deglmann and F. Furche, *J. Chem. Phys.*, 2002, **117**, 9535; P. Deglmann, F. Furche and R. Ahlrichs, *Chem. Phys. Lett.*, 2002, **362**, 511; K. Eichkorn, O. Treutler, H. Oehm, M. Haeser and R. Ahlrichs, *Chem. Phys. Lett.*, 1995, **240**, 283; K. Eichkorn, F. Weigend, O. Treutler and R. Ahlrichs, *Theo. Chem. Acc.*, 1997, **97**, 119; T. Koga and H. Kobayashi, *J. Chem. Phys.*, 1985, **82**, 1437-1439; P. Pulay, *Chem. Phys. Lett.*, 1980, **23**, 393-398; O. Treutler and R. Ahlrichs, *J. chem. Phys.*, 1995, **102**, 346; F. Weigend, *Phys. Chem. Chem. Phys.*, 2006, **8**, 1057.
23. A. Klamt and G. Schüürmann, *J. Chem. Soc. Perkin Trans. 2*, 1993, 799-805.
24. S. Grimme, J. Antony, S. Ehrlich and H. Krieg, *J. Chem. Phys.*, 2010, **132**, 154104-154104; S. Grimme, S. Ehrlich and L. Goerigk, *J. Comput. Chem.*, 2011, **32**, 1456-1465.